

AMERICAN MUSEUM NOVITATES

PUBLISHED BY THE AMERICAN MUSEUM OF NATURAL HISTORY
CITY OF NEW YORK DECEMBER 11, 1952 NUMBER 1601

THE HYDRODYNAMIC ASPECTS OF FISH PROPULSION

BY D. R. GERO¹

CONTENTS

INTRODUCTION.....	1
SYMBOLS.....	2
DRAG.....	3
THRUST.....	14
POWER LOADING.....	24
PROPULSIVE EFFICIENCY.....	28
SUMMARY.....	31
CONCLUSIONS.....	31
BIBLIOGRAPHY.....	32

INTRODUCTION

The problem of fish propulsion is a most challenging one and a problem that has been investigated only from a somewhat philosophical standpoint for many years, with no attempt directed towards a practical or engineering solution. A closer examination of the problem may partially explain this academic attitude, in that the solution is dependent on an organism the actions of which do not readily lend themselves to exact mathematical manipulations. In spite of this, certain realms of the activities of fishes² are based on the fundamental laws of hydrodynamics, kinematics, and stability which can be analyzed and evaluated objectively.

In recent years the need for obtaining additional information on bodies maneuvering in a medium the density of which is ap-

¹ Head, Applied Mechanics Section, Research and Development Department, Goodyear Aircraft Corporation, Akron, Ohio.

² Included in this study is a single species of porpoise as well as fishes. No distinction is made in the text where it is evident that one or the other is excluded from the discussion.

proximately equal to the density of the body itself has become more and more acute, particularly in the field of under-water and lighter-than-air craft. The fish performs certain functions that, if duplicated or transferred in character to under-water or lighter-than-air craft, would greatly increase the value of these craft. The subject investigation was undertaken in an attempt to determine the manner in which fish so ably perform the swimming function, and in the course of this study to determine whether or not there were any basic features that could be applied to the improvement of the types of vehicles mentioned above.

The marine phase of this investigation was conducted at the Lerner Marine Laboratory, Bimini, British West Indies. This facility was made available to the Goodyear Aircraft Corporation through the courteous cooperation of Dr. C. M. Breder, Jr., of the American Museum of Natural History, who has been most helpful during the entire program.

SYMBOLS

C_{D_T}	Total drag coefficient = total drag/ $[1/2\rho V^2 S]$
C_f	Friction coefficient
C_{D_F}	Form drag coefficient
C_{D_t}	Induced drag coefficient
R	Reynolds number
ρ	Water density, slugs/feet ³
$C_{D_{RES}}$	Residual drag coefficient
$A.R.$	Caudal fin aspect ratio = (tail span) ² /tail area
e'	Polar correction factor
l/d	Fineness ratio, body
g	32.2 feet/second ²
V_0	Free stream velocity, feet/second
h	Height, feet
C_L	Lift coefficient = $L/[1/2\rho V^2 S']$
α	Tail angle of attack, absolute
Λ	Tail sweep-back angle
α_Λ	Effective tail angle of attack for swept-back tail
$V_{0\Lambda}$	Effective tail velocity for swept-back tail
$(dC_L/d\alpha)_0$	Slope of lift curve for tail
$(dC_L/d\alpha)_\Lambda$	Effective slope of lift curve for swept-back tail
B	Buoyancy, pounds
W	Weight of fish in air, pounds
s	Linear unit distance, feet
t	Time, seconds
M	W/g , slugs
$K_m, n, \omega_1, \omega_2$	Constants

e_1	Naperian base
e	Power loading, horsepower per pound of muscle
V_T	Terminal velocity, feet/second
η	Propulsive efficiency
A	Maximum cross section area of body, feet ²
S	Total surface area of body, feet ²
C_f'	Effective friction drag coefficient
m	Per cent laminar flow
ν	Kinematic viscosity
l	Body length, feet
d	Maximum body diameter, feet
S'	Tail area, feet ²
V_N	Translational tail velocity, feet/second
V_{N_0}	Maximum translational tail velocity, feet/second
Θ	Angle between body center line and tail
Θ_0	Maximum angle between body center line and tail
w	Weight in water/weight in air
β	$\cos^{-1} V_N/V_R$
γ	$\tan^{-1} V_N/V_R$
T	Total thrust, pounds
λ	Tail taper ratio
P	Period of tail oscillation
F	Froude number = V/\sqrt{gl}
V_R	Resultant velocity, feet/second
W_m	Weight of fish muscle, pounds
q	Dynamic pressure, $\frac{1}{2}\rho V^2$, pounds/feet ²
a	Acceleration, inches/second ²
D	Displacement, inches ³
S_f	Flat plate area, feet ²
w	Per cent weight not supported by buoyancy
L	Lift, pounds

DRAG

The basic drag characteristics of the subject animals are unlike those of rigid bodies moving through air or water in that the body is flexible and is accompanied by additional drag arising from the complicated oscillatory swimming motions. The case in question here is confined to fishes and aquatic mammals that derive their propulsion primarily from their tails or flukes and not from the entire body as does the eel.

Many of the previous investigators have attempted to evaluate the drag of fish by use of rigid models, but the shortcomings of this method are quite obvious in that they have omitted the induced drag, as well as other drag components, as is explained be-

low. An entirely dynamic solution to the drag problem would be most desirable, but it entails an elaborate mathematical investigation. For purposes of analysis in this work a compromise has been reached, inasmuch as friction and form coefficients have been used for those portions of the body not contributing to the thrust, and induced coefficients have been used for determining the drag of those parts furnishing the thrust. In other words, the main body and auxiliary fins are considered to contribute drag in accordance with conventional form and friction coefficients, while the caudal fin or main propulsive fin contributes an induced drag resulting from the dynamic oscillations of the tail itself.

The total drag may be considered as the sum of the drag from the surface area of the fish, the physical configuration of the fish, and the induced drag of the tail associated with its oscillatory motion. This, according to normal convention, can be expressed as:

$$\begin{aligned}
 C_{D_T} &= C_f + C_{D_F} + C_{D_i} && (1) \\
 C_f &= 4.55 / (\log_{10} R)^{2.48} && \text{Turbulent skin friction coefficient; von Mises (1945)} \\
 C_f &= 1.328 / \sqrt{R} && \text{Laminar skin friction coefficient; von Mises (1945)} \\
 C_{D_F} &= (\text{Empirical}) && \text{Form drag coefficient} \\
 C_{D_i} &= C_L^2 / \pi A \cdot R \cdot e' && \text{Induced drag coefficient; von Mises (1945)}
 \end{aligned}$$

The friction drag coefficient, C_f , is a function of the surface condition of the fish and velocity of water relative to the body of the fish. C_f for this study has been assumed to be the same as for a smooth rigid body, since for all practical purposes the areas of the body on which this coefficient is based have relatively small oscillatory motion during swimming. As is indicated above, there are two basic types of flow to be considered in connection with the friction coefficient, one laminar and one turbulent (see fig. 1). These values are determined on the basis of Reynolds number which is a function of the velocity of fish, basic linear dimension of the body, and the kinematic viscosity of the medium. There is an intermediate or transition regime where neither the laminar nor the turbulent coefficient applies directly. The characteristics of this regime are determined experimentally and can be expressed by empirical equations similar to the ones developed for use in the Power Loading section of this study, below.

The form drag coefficient, C_{D_F} , does not readily lend itself to exact equations, and it has been the experience of those people working with such bodies as are here considered that certain errors are found which are involved in transforming the normal C_f based on a flat plate to a body of three dimensions. As a result of this an additional term, residual drag coefficient, $C_{D_{RES}}$, has been used to include the C_f conversion error and the C_{D_F} form drag of the body. This information has been compiled from a

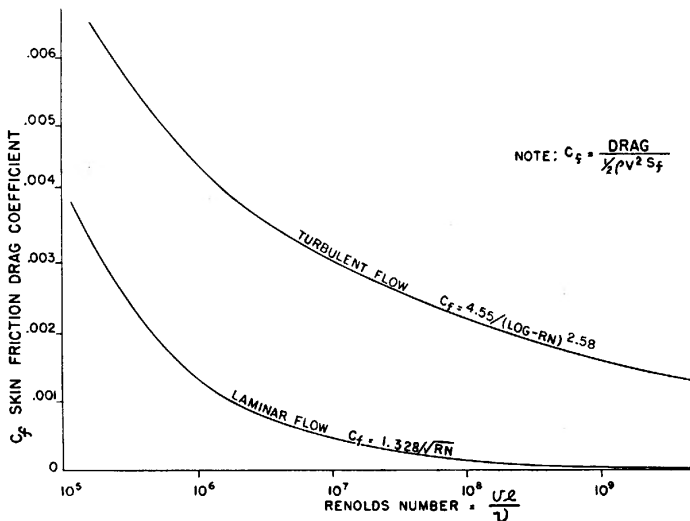


FIG. 1. Variation of skin friction drag coefficient, C_f , with Reynolds number for flat plates.

considerable amount of past experience with this problem, in addition to the results of wind-tunnel test data. Figure 2 represents a typical curve of $C_{D_{RES}}$ versus fineness ratio, l/d , for turbulent flow, where

$$C_{D_{RES}} = \Delta C_f + C_{D_F} \quad (2)$$

Another item that must be considered in connection with the drag of the subject bodies is the wave-making resistance which, under certain critical conditions, increases the residual drag to many times its normal value. This is expressed as a function of Froude number which is V_0/\sqrt{gl} . Figure 3 represents the manner in which the residual drag might be increased for certain Froude numbers with (depth/diameter) as a parameter.

The drag contributed by the caudal fin is associated with the oscillatory motion of the fin and is of an induced nature.

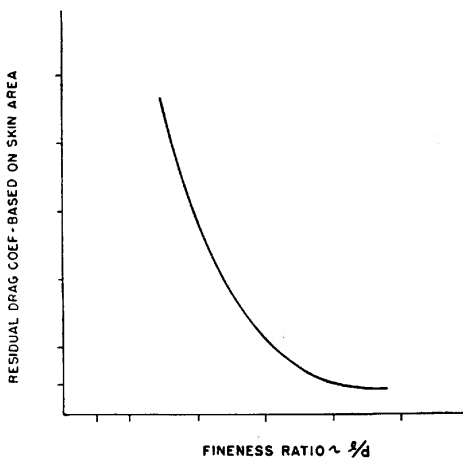


FIG. 2. Body residual drag coefficient versus fineness ratio for turbulent flow.

This drag physically manifests itself as turbulence in the wake of the fish and is lost energy in a sense. The induced drag is a function of the lift, C_L , or thrust coefficient in this case, and

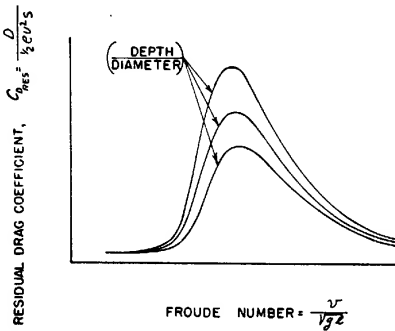


FIG. 3. Body residual drag coefficient versus Froude number, with (depth/diameter) as a parameter. This figure illustrates the divergence of the drag coefficient in the critical Froude number region.

A.R., aspect ratio of the caudal fin. In the subsequent analysis, values of induced drag have been obtained by using the resultant mean velocity of the caudal fin during its oscillatory motion.

The significance of the induced drag term can be illustrated by pointing out that, for a given C_L , as the aspect ratio, $A.R.$, of the tail increases the associated induced drag decreases. Scombrid-form fishes such as the tuna or wahoo, by virtue of their high tail $A.R.$, are accompanied by low induced drag, whereas the barracuda must have a high induced drag.

One aspect of the configuration of the fish that has not been considered is the effect of the sweep-back of the caudal fin on the induced drag.

In normal high-speed aerodynamics the effect of sweep-back is fairly well defined. The net result of sweep-back consists of a reduction in the velocity of flow across a section normal to the

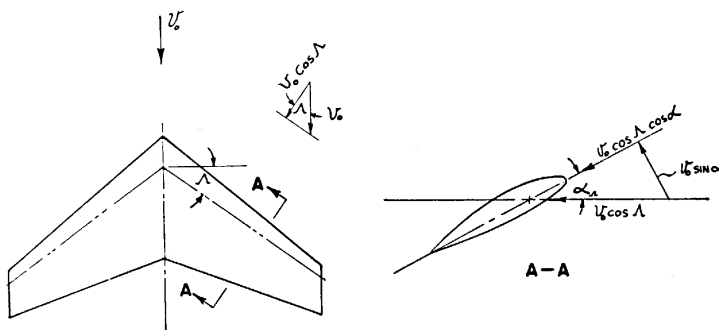


FIG. 4. Influence of sweep-back on the velocity over the caudal fin.

leading edge (or 1/4 chord line) and an over-all decrease in the slope of the lift curve.

This has an interesting implication in connection with the flow across the tail of the fish in that the velocity is reduced and the resulting local pressure is thereby increased, a fact that could discourage the onset of cavitation. The influence of sweep-back as applied to the present discussion is best illustrated by figure 4.

From this analysis it is apparent that the effective angle of attack α_A has increased and V has decreased. $(dC_L/d\alpha)_A$ is smaller than for normal unswept surfaces, and it appears for a given α that the induced drag should also be smaller since:

$$C_{D_i} = C_L^2 / \pi A.R.e' = [(dC_L/d\alpha)_A \alpha]^2 / \pi A.R.e' \quad (3)$$

This brings to light another interesting aspect of induced drag

in connection with the effect of the flexible trailing edge on the wake of the fish, particularly on the Karman street. As the fluid passes aft over the body of the fish the microscopic layer next to the body is retarded and lags behind the fluid at some distance from the body. Certain energy is stored in the fluid next to the body of the fish, the body actually dragging this liquid forward, relatively speaking, through the rest of the fluid. If the body were rigid, as the fluid passed by the trailing edge a series of vortices would be set up, the energy of which would be equal to the energy imparted to the liquid by the body of the fish. However, it is possible that the flexible portion of the tail is active in developing a favorable pressure gradient which permits a larger area of laminar flow to exist so that the above losses are minimized and the resultant drag is reduced. Effectively, this could be accomplished by the fact that the flexible tail trailing edge presents a large radius corner around which the fluid can flow. Any reduction in the drag of this nature would be extremely important, since the skin friction drag represents a large percentage of the total drag. From actual observations of fish wake in Bentonite it was noticed that the tips of the caudal fin produced less turbulence than the center portion of the fin. A large volume of water appeared to flow past the center section of the caudal and not so much past the tips.

Bentonite as used here is a colloidal suspension of Bentonite clay in water. This suspension is sensitive to velocity gradients and when viewed through a polariscope renders a visible fringe pattern around any body moving through the liquid. This liquid has been used for analyzing flow patterns qualitatively and can be used as a quantitative tool by employing the photo-viscous method of flow analysis.

Hill (1949) indicates a very pointed example of the physical nature of the wake by stating that a porpoise, an efficient swimmer, when viewed at night during the period when the sea contains a high concentration of phosphorescent Protozoa, leaves a very thin luminous trail representing a minimum disturbance. However, in the case of a seal the wake left is very luminous and disturbed, representing a large turbulent disturbance.

In order to evaluate the various drag values properly, an extensive series of tests were set up and conducted in the Hydrodynamic Laboratory of the Goodyear Aircraft Corporation. These tests consisted of dropping a large number of fish in a

vertical drop tank. This drop tank was approximately 7 feet high and 2 feet by 2 feet in section, one side of which had a clear plastic front cross-hatched with 2-inch squares. This served as a gridded background and made it possible to determine the velocity of the fish dropped in the tank by analyzing the motion pictures taken of the fish during the drops. The use of a tank this small for conducting drop tests could be questioned owing to the effect of wall interference and the restricted drop height. However, for the purpose at hand it appears to have provided satisfactory results, since it was possible for the fish to reach a stabilized terminal velocity condition.

A large variety of fresh-water fish was obtained in order to evaluate properly the effect of fineness ratio. The weight characteristics for several of the fish tested are listed in table 1. The

TABLE 1
FRESH-WATER FISH CHARACTERISTICS

	Weight in Air (Grams)	Weight in Water (Grams)
Perch, <i>Perca flavescens</i> (Mitchill)	92.8	0
Perch, <i>Perca flavescens</i> (Mitchill)	128.2	0.3
Dogfish or bowfin, <i>Amia calva</i> (Linnaeus)	1159	81.7
Catfish, <i>Opladelus olivaris</i> (Rafinesque)	169	0
Garfish, <i>Lepisosteus osseus</i> (Linnaeus)	399	67.5

drop tests were performed by harmlessly electro-narcotizing the fish for a short period, as described by Okada (1929), suspending the fish in the water at the top of the tank, and releasing the fish at a predetermined signal. At this signal motion pictures were taken of the drop from which, on further analysis, a time-versus-distance curve was obtained. A single differentiation was performed on this curve to obtain the terminal velocity, and hence the terminal drag could be determined. This condition simplified the drag analysis, since in the terminal condition the drag is exactly equal to the net weight of the fish in water. This becomes evident on examination of figure 5.

$$\begin{aligned} \text{Net accelerating force} &= W - D - B \\ W - D - B &= (W/g)d^2s/dt^2 \\ D &= (W - B) - (W/g)d^2s/dt^2 \end{aligned} \quad (4)$$

At the terminal condition $d^2s/dt^2 = 0$ and $D = W - B$ which is the net weight of the fish in water. All (W/g) values should be increased by approximately 10 per cent to include the additional mass of water that is carried along by the body of the fish.

The net weight was precisely determined by weighing the fish in and out of the water prior to the drop test. Since the terminal velocity was a function of the weight of the fish, it was possible to obtain several points on a C_{D_T} versus Reynolds number curve by ballasting the fish without changing the external configuration. It would appear that C_{D_T} is independent of fineness ratio since the catfish (*Opladelus*) ($l/d = 3$) and the garfish (*Lepisosteus osseus*) ($l/d = 14$) had approximately the same drag coefficients.

The surface condition was investigated by constructing the control model of an N-type airship (fig. 6) and conducting identical drop tests as in the case of the fish. The weight of this model

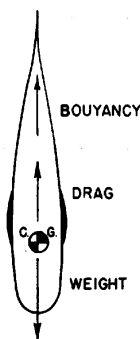


FIG. 5. Free body diagram of fish during drop test.

was 1170 grams in air and 170 grams when completely submerged in water. The model was first dropped dry, and a drag value was determined at terminal velocity. The mucus from a dogfish (*Amia calva*) was then liberally applied to the model, and the drop was repeated. The application of the mucus rendered no reduction in drag, but there was a slight increase in the directional stability.

Since the normal scatter of the initial test points rendered an exact second differentiation impractical, a method was devised by William C. Johnson of Goodyear Aircraft whereby a theoretical equation was made to fit the original time-versus-distance curve. The basic equation was as follows:

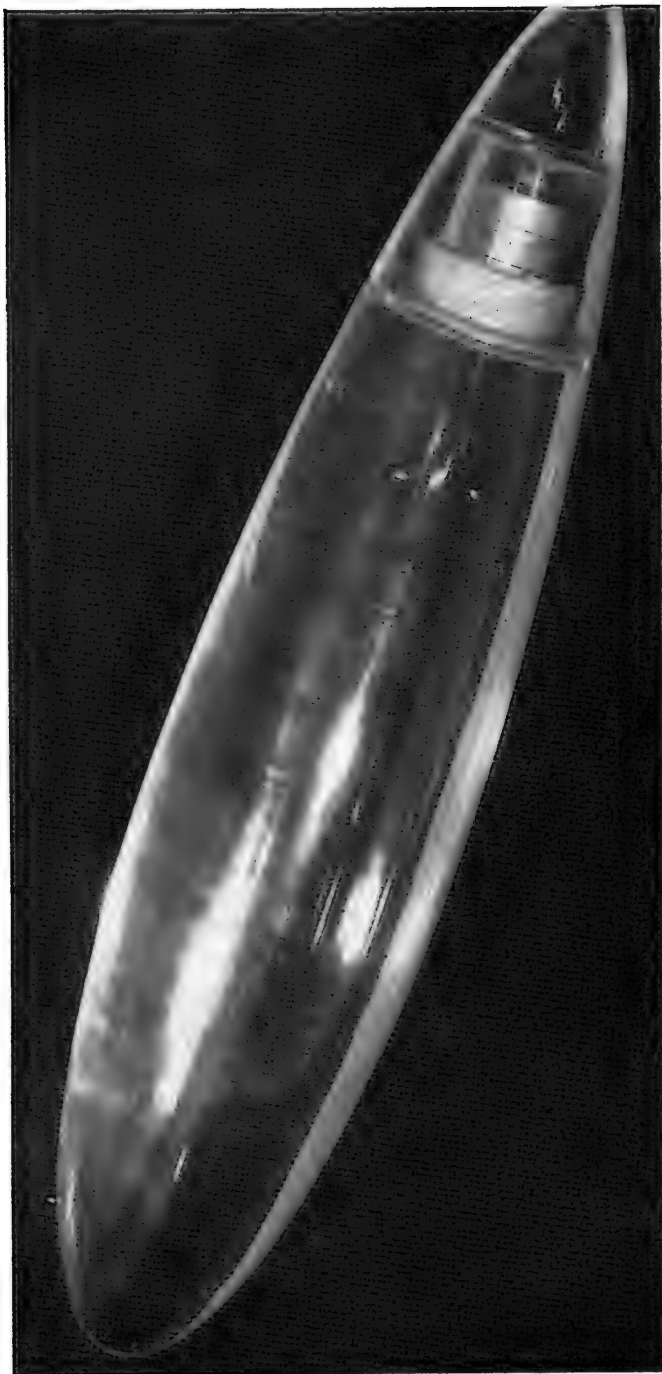


FIG. 6. Drop test model of N-type of airship without fins. Fins were deleted for drag investigation of bare hull.

$$M \frac{dv}{dt} + K_m V^n = \omega Mg \quad (5)$$

Two solutions of this equation can be found in any standard text (Cohen, 1933) which are:

$$\frac{d^2s}{dt^2} = \omega g e_1 - \omega g t/V \quad (n = 1) \quad (6)$$

$$\frac{d^2s}{dt^2} = \omega g \operatorname{sech}^2 \omega g t/V \quad (n = 2) \quad (7)$$

Equation 6 represents the condition $R = 0$ to $R = 100,000$ where it was assumed that the drag coefficient varied as V to the first power.

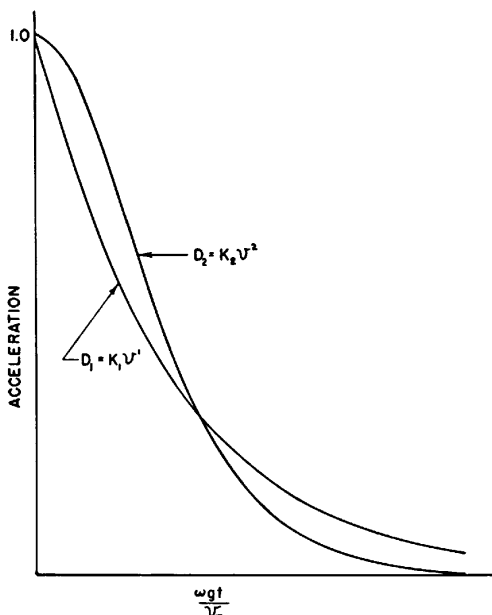


FIG. 7. Basic theoretical acceleration curves used for determining the drag of fresh-water fish. This information was used in conjunction with the results of the drop test of fresh-water fish. See text for derivation and explanation.

Plots of these two equations are presented in figure 7. The exact mechanics of applying this equation to the experimental time-versus-distance curve consisted of first assuming a terminal velocity, V_t , and performing a double integration to arrive at a theoretical time-versus-distance curve which would fit the original data. By a series of trials in choosing different V_t values, it was possible to obtain a reasonably accurate approximation to the original data. It should be noted that the original information had to be corrected for zero time, since the film record

may have started between frames on the recording camera. Figure 8 represents the results of a typical operation of this type for a dogfish (*Amia calva*) with the following characteristics:

$$\begin{aligned} W_{\text{air}} &= 2.76 \text{ pounds} \\ W_{\text{H}_2\text{O}} &= 0.463 \text{ pound} \\ D &= 66.5 \text{ inches}^3 \\ a &= 62.0 \text{ inches/seconds}^2 \\ V_T &= 69.0 \text{ inches/seconds} \end{aligned}$$

The findings of the Goodyear Aircraft Corporation tests, which indicate that the mucus apparently caused no reduction in drag, verified the work of Richardson (1936) who dropped fish models

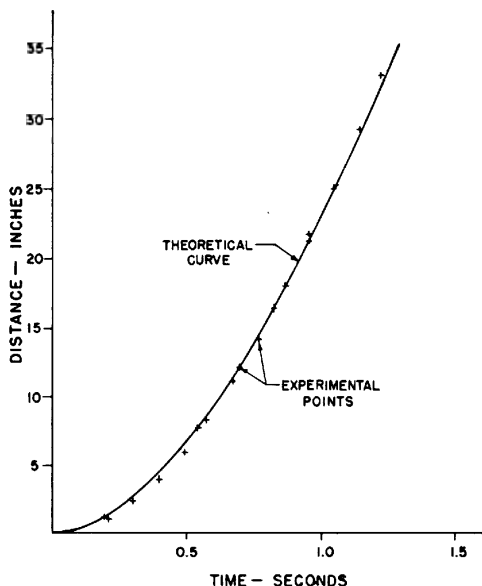


FIG. 8. Theoretical curve fitted to experimental points for dogfish drop test. Successive differentiation of this theoretical curve with respect to time provides accurate velocity and acceleration information.

having different surface conditions and found that a highly polished model actually had lower total drag than the similar fish body. He further proved his point by checking the common face of two fluids, coal oil (kerosene) and water, using a hot-wire anemometer, and found that there was no discontinuity in the velocity at the interface, and hence no slippage. Therefore, it seems to have been proved conclusively that (1) there is no

reduction in drag of a fish surface over a polished surface, since there is no slippage between the two liquids (water and mucus); and (2) since the fish cannot generate sufficient mucus to act as a track, the mucus must serve some purpose other than minimizing the drag.

Dr. Breder of the American Museum of Natural History (personal communication) states that "it is well known to physiologists that this mucus has an important role in maintaining the physiological integrity of the fish by modifying the osmotic characteristics of the skin. This is probably the most important function it has."

THRUST

Although there are many different ways in which fish may propel themselves, for purposes of simplicity only one type, the carangiform (Breder, 1926), was investigated. The primary reason for this choice lay in the fact that all the larger fish investigated obtained their thrust from this type of motion.

In the carangiform motion the thrust is assumed to be provided by the posterior section of the body of the fish, principally the caudal fin. The basic movement is characterized approximately by the superposition of a rotational velocity onto a translational lateral velocity of the tail.

As is well known, it is possible to obtain thrust from an airfoil or hydrofoil in a free stream by simply oscillating the surface in a direction normal to the stream velocity.

Figure 9 represents a surface which is moving normal to free stream velocity, V_0 , with a transverse velocity equal to V_N . A rotational velocity is superimposed on this condition which permits the surface to acquire some angle γ with respect to the direction of the free stream. If the rotational component is removed and γ is reduced to zero, it is possible, as shown below, to obtain a thrust component which provides a forward propelling force:

$$\begin{aligned} V_R &= \sqrt{V_0^2 + V_N^2} \\ L &= \frac{1}{2}\rho V_R^2 (dC_L/d\alpha)\alpha S \\ T &= \frac{1}{2}\rho V_R^2 (dC_L/d\alpha)\alpha S \cos \beta \end{aligned} \quad (8)$$

since

$$T = L \cos \beta$$

However, equation 8 as derived represents only the simplest case of pure translation motion normal to a free stream V_0 .

The actual complete mathematical representation of the motion of the caudal fin would include such items as variable camber and viscous damping which are in this case difficult to evaluate and for purposes of simplicity are omitted. This is not to imply that they are of minor importance but that they will require considerable future investigation to be justly treated.

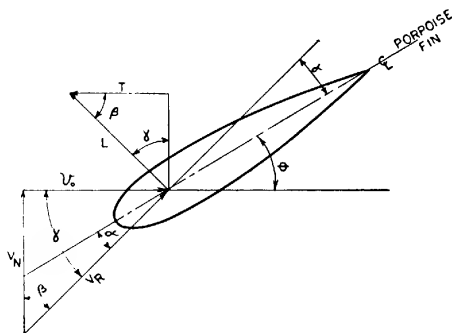


FIG. 9. Velocity diagram of caudal fin as used in basic hydrodynamic analysis.

In an attempt to approach the actual case the simple expression above has been extended by incorporating the rotational component on the translation component and using the correct simple harmonic expressions. This condition is more nearly represented by figure 9 than was the condition for equation 8.

The derivation of the composite thrust is as follows:

$$\begin{aligned}
 V_N &= V_{N_0} \sin \omega_1 t \\
 \Theta &= \Theta_0 \cos \omega_2 t \\
 \omega_1 &= \omega_2 = 2\pi/P \\
 V_R &= \sqrt{V_0^2 + V_N^2} = \sqrt{V_0^2 + V_{N_0}^2 \sin^2 2\pi t/P} \\
 \cos \beta &= V_N / V_R = V_{N_0} \sin 2\pi t/P / \sqrt{V_0^2 + V_{N_0}^2 \sin^2 2\pi t/P} \\
 \alpha &= \gamma - \Theta = \tan^{-1}(V_{N_0} \sin 2\pi t/P / V_0) - \Theta_0 \cos 2\pi t/P \\
 T &= \frac{1}{2} \rho S \sqrt{V_0^2 + V_{N_0}^2 \sin^2 2\pi t/P} (dC_L/d\alpha) [\tan^{-1}(V_{N_0} \sin 2\pi t/P / V_0) - \\
 &\quad \Theta_0 \cos 2\pi t/P] (V_{N_0} \sin 2\pi t/P) \quad (9)
 \end{aligned}$$

Owing to the lack of detail values for the limits of such values as V_{N_0} , Θ_0 , and α , it is not possible at this time to obtain accurately and quantitatively the exact variation of T with t , or stroke. In order to determine the constants and limits for equation 9, confirmation must be obtained from additional tests on amplitude of tail stroke, frequency of stroke for various V_0 values, and

actual tail angles with body during stroke. As can be seen, this is a task of no small magnitude when it is considered that only those values obtained under actual swimming conditions will be of any real value in evaluating propulsive efficiency. Figure 10 represents a typical graph of T versus t during one-half of a hypothetical stroke obtained by using equation 9.

To return to the simpler form of equation 8, it is important to notice that it is possible to obtain analytically very large thrust values under conditions simulating actual porpoise maneuvers. A family of curves (fig. 11) represents the theoretically available instantaneous thrust of a porpoise, with the characteristics

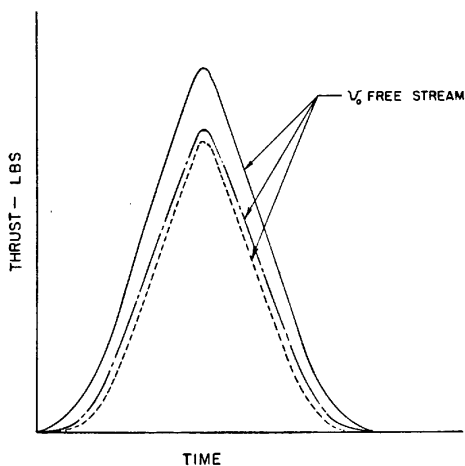


FIG. 10. Theoretical variation of thrust with time for one complete cycle of sample caudal fins using free stream velocity, V_0 , as a parameter.

below. The limits of $\alpha = 40^\circ$ and $V_{N0} = 40$ feet/seconds have been imposed as a result of preliminary studies conducted at Goodyear Aircraft Corporation and need further substantiation, as is mentioned above. These limiting values could be reduced arbitrarily and still enable the particular fish or aquatic mammal in question to obtain large thrust values. This is quite obvious from examination of figure 11 which indicates that it is possible to obtain instantaneous values over 900 pounds.

The foregoing analysis has been made in connection with the salt-water phase of the Goodyear Aircraft fish propulsion program carried on at the Lerner Marine Laboratory at Bimini. The primary purpose of this phase of the marine study was to

determine whether or not it was possible for the conventional equations and coefficients to satisfy certain remarkable maneuvers being performed by the porpoise (*Tursiops truncatus* Montague) at the laboratory.

A typical operation consisted of a porpoise performing the well-known maneuver of starting from a stationary vertical attitude and leaping from the water to feed. This maneuver should not be construed to be the same as that observed when the porpoise is swimming along with a boat and "playfully" leaps from the water. By careful observation of the porpoise during feeding,

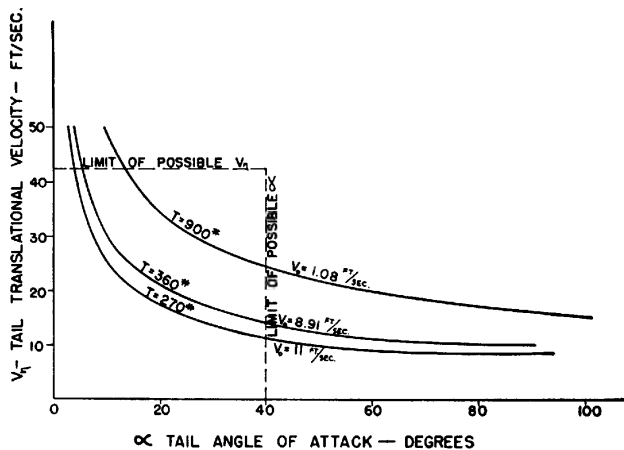


FIG. 11. Theoretical thrust developed by porpoise during maneuvers. Boundary condition of tail angle of attack and translational tail velocity limit permissible operation to that area under dotted lines. See text for derivation and explanation.

it becomes obvious that there is no "running-jump," but that the porpoise swims to a near "dead stop" in a vertical nose-up attitude from which the leap is started.

The following values were taken from a typical maneuver:

l	= 8.2 feet
W	= 400 pounds
S'	= 0.82 feet ²
$A.R.$	= 2.5
h	= 7.0 feet, height of leap
t	= 0.8 second, time to top of leap
Λ	= 30°
λ	= 0.5

The geometrical and weight values are approximations, since it was not possible to handle the porpoise.

With a reference scale as a background, motion pictures were taken during this maneuver and subsequently were analyzed. Figure 12 represents the summarized results of required tail thrust versus time. The solid line represents the product of the porpoise mass times the acceleration taken from the photographic records. The dotted line represents the thrust (equation 11) that the tail had to produce, which must be larger than the solid line since the tail was required not only to accelerate the mass of the porpoise but also to support the static difference

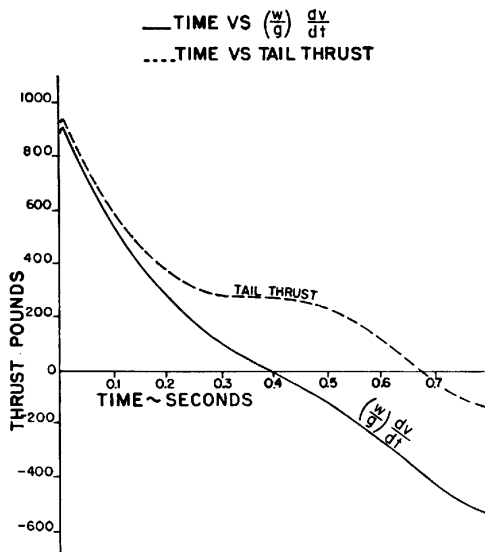


FIG. 12. Actual porpoise thrust developed during maneuver. Maximum thrust corresponds to values given in figure 11.

between the weight and the buoyant force. This can be illustrated by an expression similar to equation 4 where:

$$T + B - W = (W/g) dV/dt \quad (10)$$

$$T = (W/g) dV/dt + (W - B) \quad (11)$$

This information has been corrected for the transient buoyant force present as the body progresses out of the water.

Examination of the dotted curve (fig. 12) reveals that for the porpoise to raise himself to the height recorded in the given time

it was necessary for the tail to produce a thrust of approximately 950 pounds. From a comparison of this value with the values in figure 11 it appears that it is entirely feasible to substantiate this thrust by using known concepts.

During the fresh-water phase, a study was made using a small perch, *Perca flavescens* (Mitchill), with the following general characteristics:

$$\begin{aligned} W &= 0.24 \text{ pound} \\ T_{\text{Gross}} &= 1.2 \text{ pound} \end{aligned}$$

This experiment was performed by taking high-speed motion pictures, bottom view, of the subject perch in the Goodyear Aircraft Corporation water channel. The fish was permitted

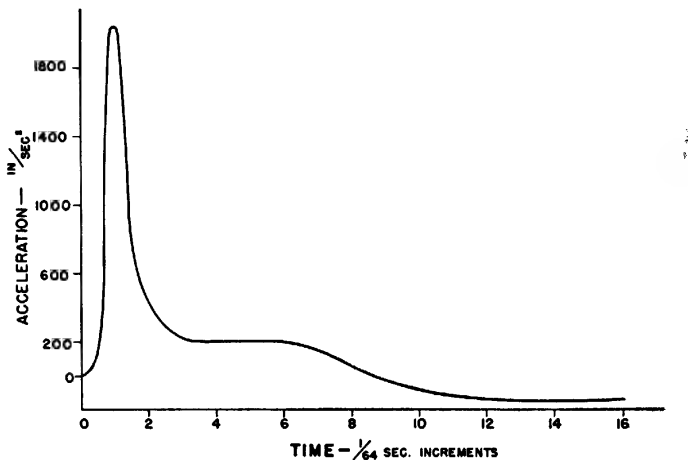


FIG. 13. Actual perch acceleration developed during maneuver.

to become acclimatized in the channel for several days and was photographed during the test under natural lighting conditions. The fish was startled from rest by the investigator's giving the side of the channel a sharp slap, at which time the perch swam rapidly from one side of the tank to the other. The motion pictures of this maneuver were analyzed, summarized, and the resulting acceleration was plotted in figure 13 as acceleration versus time. The resulting power loading is equal to 0.0385 horsepower/pound of muscle. There has been a considerable amount of work done on this particular phase, with some of the work quoting values as low as 0.010 horsepower/pound (Gray, 1948). This appears to be a very crude and approximate value

to be used for such important purposes, since it is based, according to Parry (1948), on the total work done during a 15-minute maximum effort of a rowing crew. It goes without saying that investigations should be started immediately to determine accurately what this value should be from a physiological standpoint. Parry and Gray both feel, as the author does, that this value is exceptionally low. Parry has referred to the work of Dickinson (1928), in which it is shown that a man can develop 0.02 horsepower/-pound of muscle and states: "this suggests that an animal capable of a higher rate of oxygen intake than man might develop greater power for a given time or a given power for a greater time. This idea is supported by the observation of Scholander (1940), on a porpoise that both the vital capacity (relative to man) and the absorption constant were greater than in man." The full significance of power loading is explained in a later section of the text.



FIG. 14. Installation of piscatometer in the launch at Lerner Marine Laboratory at Bimini.

During the second, or marine, phase of this extended research program, an instrument called a piscatometer was devised for measuring the actual net horsepower available. As shown installed in the fishing craft in figure 14, this equipment consists of two separate and independent systems: a load system and a velocity system.

This instrument was mounted in the launch and was equipped with the standard fishing tackle as illustrated in figure 15. Large

salt-water fish were caught in the conventional manner and, by means of a remote acting camera and gauges, the thrust and velocity activities of the fish were recorded on a permanent record for further study.

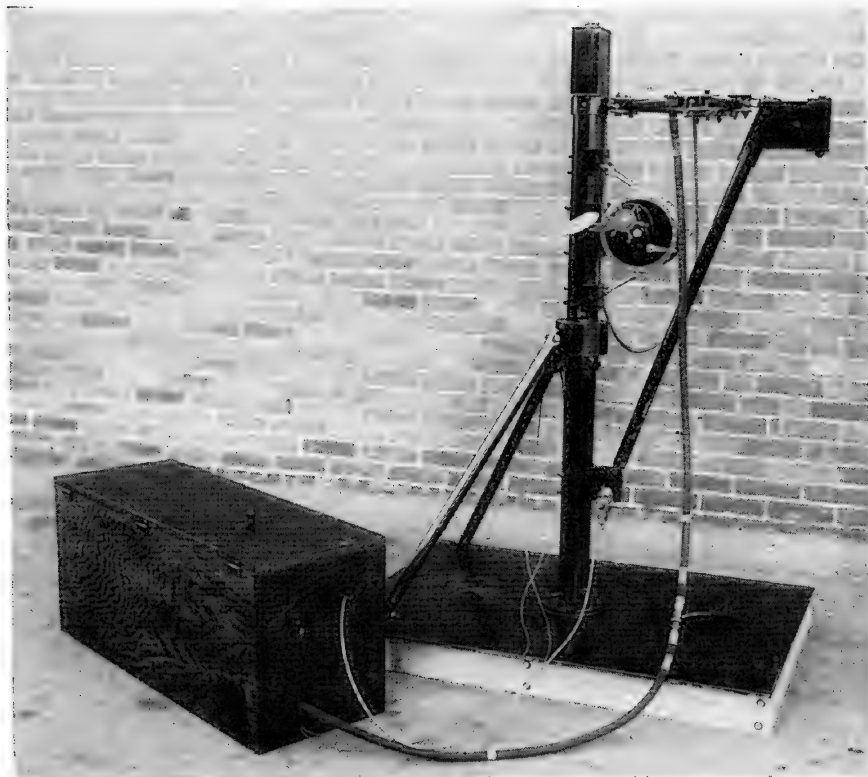


FIG. 15. Piscatometer, a remote indicating device used for the determination of thrust, velocity, and horsepower of large salt-water fish.

The tension in the line was measured indirectly by a hydraulic strut inserted in the "diamond" linkage which connected the boom to the main upright. The pressure was transmitted to the instrument box where it was registered on a meter. The velocity of the line was determined by running the line over a pulley installed on the axis of the lower boom support; this pulley in turn drove a tachometer. The tachometer was connected to an indicator in the instrument box by flexible cable.

Table 2 summarizes the characteristics of the particular fish investigated with the use of the piscatometer.

TABLE 2
SALT-WATER FISH CHARACTERISTICS

	Test No.	Weight in Air (Pounds)	Weight in Water (Pounds)	Length (Inches)	One-half Girth (Inches)	Maximum Thrust (Pounds)	Maximum Speed (Feet/Second)	Maximum HP.
Shark No. 1, <i>Carcharhinus lucas</i> (Müller and Henle)	3	58.0	3.5	60.0	—	22.6	17.1	0.26
Shark No. 2, <i>Carcharhinus lucas</i> (Müller and Henle)	4	21.0	2.0	—	—	16.0	13.3	0.125
22 Grouper No. 1, <i>Promicrops itaiara</i> (Lichtenstein)	5	17.0	0	—	—	46.0	5.7	0.115
Grouper No. 2, <i>Promicrops itaiara</i> (Lichtenstein)	6	41.0	2.0	43.25	13.5	—	—	—
Shark No. 3, <i>Carcharhinus lucas</i> (Müller and Henle)	7	19.0	2.0	42.0	9.5	—	—	—
Shark No. 4, <i>Isurus oxyrinchus</i> Rafinesque	15	71.0	4.0	67.5	15.0	—	—	—
Shark No. 5, <i>Negaprion brevirostris</i> (Poey)	19	81.0	3.0	72.5	13.0	38.4	8.0	0.38
Shark No. 6, <i>Negaprion brevirostris</i> (Poey)	20	58.5	3.5	67.0	12.0	34.8	—	—
Barracuda, <i>Sphyraena barracuda</i> (Walbaum)	24	20.0	1.0	48.0	9.25	38.0	40.0	0.81
Barracuda, <i>Sphyraena barracuda</i> (Walbaum)	26	25.0	0.5	51.0	9.75	19.0	40.0	0.525

Figure 16 represents the type of information secured from the equipment and indicates the general character of the remaining fish information.

The maximum velocity was obtained by declutching the reel and permitting the fish to run free. The other points along the force curve were obtained with varying amounts of drag on the reel up to fully tight. The maximum thrust on this curve and for all other curves, except for the very slow grouper, occurs at some point between zero speed and maximum speed. At zero speed the fin is probably "stalled out," while at maximum speed there

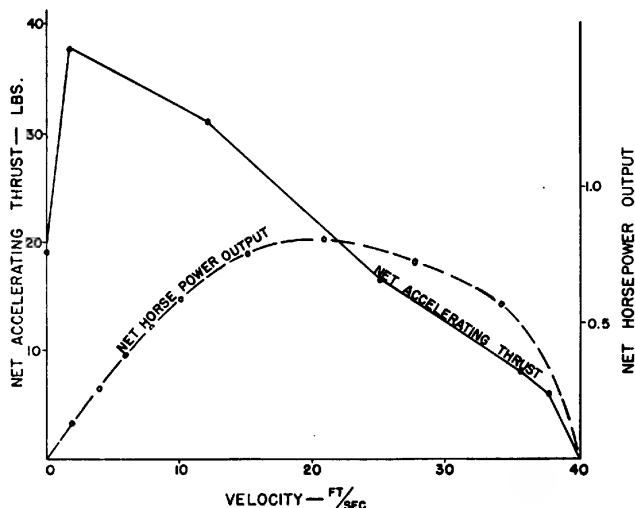


FIG. 16. Typical thrust, velocity, and horsepower information obtained from barracuda no. 24, with equipment shown in figure 14.

is no available accelerating thrust left, as it is being entirely used for propelling the fish through the water.

This information represents only the net accelerating force over and above that required to propel the fish through the water. Experimental attempts at determining the intrinsic drag of these fish have been unsuccessful. One question that could rightfully be asked is, to what extent did the hook and line interfere with the native swimming characteristics of the fish? This interference, of course, cannot wholly be discounted, but it was possible, while recording the information, to record only when the fish was swimming directly away from the boat; i.e., no side load on the forward section of the fish. In addition to this, even

though the forward section was restrained, it does not appear to be too serious because only the aft 25 per cent of the body provided the entire thrust.

POWER LOADING

The forward thrust produced by the subject animals represents only the forward component of the total force developed by the tail. The energy available from this action is less than the total energy expended by the fish, depending on the propulsive efficiency of the particular tail configuration.

The term propulsive efficiency as used here is a rather elusive expression but has been defined as the efficiency of the tail in converting tail energy into forward energy, with no considerations given to the thermal efficiency of converting food energy into mechanical energy. Although the thermal aspect has been considered in other studies, it is a physiological proposition and has not been pursued in this study.

As in the case of conventional engine nomenclature, it is convenient and appropriate to express the power of the "fish power plant" in terms of horsepower per pound of engine, or muscle. It has been determined that the muscular weight of the particular type of animals in question represents approximately 20 per cent of the total weight of the fish, a value that is used throughout the remainder of the investigation.

Since, in the steady-state condition, the power required by the fish is proportional to the drag and inversely proportional to the propulsive efficiency, the practical expression of power loading e as horsepower per pound of muscle becomes

$$e = DV/550\eta W_m \quad (12)$$

where the total drag is

$$D = \frac{1}{2}\rho V^2 C_{DT} S \quad (13)$$

C_{DT} includes all drag terms reduced to the surface area of the fish and is represented as

$$C_{DT} = C_{DF} + C_f + C_{Dt} \quad (14)$$

Previous calculations and available references indicate that for high Reynolds numbers and for C_{DT} and C_f based on the same representative area, equation 14 can be simplified to

$$C_{DT} = 1.22C_f \quad (15)$$

Substituting equations 13 and 15 into the original expression 12, we find that

$$e = 0.00214 V^3 S C_f / \eta W_m \quad (16)$$

The C_f term in its original form, as frictional drag coefficient does not completely satisfy the purpose at hand, since the present study is directly concerned with the character of flow and not simply a singular drag value at a particular Reynolds number.

Therefore, a new and more appropriate expression, C'_f , has been introduced, which permits a more accurate interpretation of the flow conditions present:

$$C'_f = (1 - m/100)C_{f_T} + m/100C_{f_L} \quad (17)$$

where

m = per cent laminar (100%, 50%, etc.)

C_{f_T} = turbulent friction coefficient for particular Reynolds number

C_{f_L} = laminar friction coefficient for particular Reynolds number

If C'_f be substituted for C_f in equation 16, the total expression then becomes

$$e = [0.00214 V^3 S / \eta W_m] [(1 - m/100)C_{f_T} + m/100 C_{f_L}] \quad (18)$$

Thus equation 18 presents a convenient means of representing the relationship between power loading required and flow or frictional drag character of a particular body under various conditions.

To digress briefly, it should be pointed out that as a result of the author's examination of past methods of determining the drag of the subject animals, and subsequently power, no consideration had been given by others to any form of resistance except friction drag. Even though this value is important, and in most cases represents 60 to 80 per cent of the total drag, a serious error can be made by neglecting all other forms of resistance.

The most important drag terms that have been neglected are:

1. Induced drag, which is associated with the oscillatory motion of the tail of the fish and manifests itself as lost energy or turbulence in the wake.
2. Residual drag is composed of two separate terms: (a) form drag, C_{D_F} , which results from the three-dimensional character of the body, and (b) a secondary correction, ΔC_f , of the friction drag which results in transferring from a flat plate to a three-dimensional body.

3. Froude number effect on the residual drag, as is mentioned above, can under certain maneuvering conditions create large discrepancies in the total drag (see fig. 3). This effect becomes critical for relatively low values of (depth/diameter), and it should be given careful consideration, since estimated speeds and consequently horsepower estimates have been made by observing the fish in relatively shallow water where conditions accompanying low (depth/diameter) ratios are in effect.

By way of illustration, consider the values for the whale given by Hill (1949) as expanded by the author below:

$$\begin{aligned}
 l &= 84 \text{ feet} \\
 W &= 200,000 \text{ pounds} \\
 A &= 2800 \text{ feet}^2 \\
 V_0 &= 15 \text{ knots} \\
 R &= 1.25 \times 10^8 \\
 F &= 0.484 \\
 l/d &= 7.00 \text{ (approximately)} \\
 h/d &= 1.70 \text{ (approximately)}
 \end{aligned}$$

Examination of these values reveals that the Froude number of 0.484 at 15 knots is in the critical region for bodies of fineness ratio 7.00. This results in an increase of $C_{D_{RES}}$ many times the normal value and will obviously require a considerable increase in the calculated horsepower available.

To return to equation 18 in order to illustrate its real meaning, three large marine animals were investigated, the general geometric characteristics of which are presented in the following section.

The first of the three animals investigated was the porpoise studied by the author at Bimini. The second was the dolphin described by Gray (1936). The third animal was not so large as the two preceding ones but was more completely studied, since it was possible by means of the special mechanical rig (see fig. 15) to determine the actual net available thrust and maximum terminal velocity. The general characteristics of this animal, a barracuda (*Sphyraena barracuda*), are as follows:

$$\begin{aligned}
 l &= 4.0 \text{ feet} \\
 W &= 20 \text{ pounds} \\
 W_m &= 4.0 \text{ pounds} \\
 T &= 38 \text{ pounds} \\
 V_0 &= 40 \text{ feet/seconds}
 \end{aligned}$$

Figure 17 represents a summary of the information obtained

for the porpoise and dolphin, using equation 18, and is presented as power loading versus velocity for various percentages of laminar flow. Since the present work has not proceeded to the point of determining actual propulsive efficiency values, η has been assumed to be 1.00. This is conservative, and linear adjustments will be required when the actual values are eventually known.

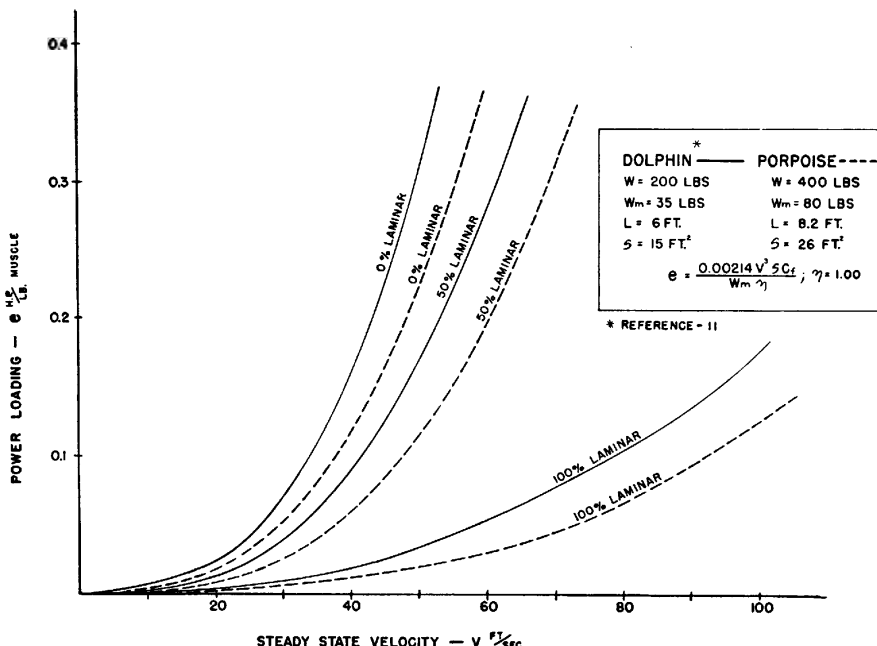


FIG. 17. Power loading versus steady-state velocity for two representative subjects, with per cent laminar flow as parameter. See text for derivation and explanation.

Upon examination of figure 17, several interesting observations can be made. In the first place the slopes of the curves decrease with increase in body size. This is to be expected since

$$e = \text{power/weight} \approx l/(\text{weight})^{1/2}$$

This can be seen from the fact that for geometrically similar bodies the required horsepower varies as the surface area, and the weight of muscle varies approximately as the weight or displacement of the body. Second, from figure 17, for presently accepted values of e in the order of 0.01, it is apparent that for

reasonable values of velocity (40 feet/seconds) the flow must be approximately 100 per cent laminar. This appears to be too optimistic. However, it does appear, as has been substantiated by the following information on the barracuda, that values of e greatly in excess of 0.01 can be obtained.

It would appear on the basis of this that a compatible solution would be obtained with values of e in the order of 0.10 and corresponding drag values approaching 50 to 75 per cent laminar flow.

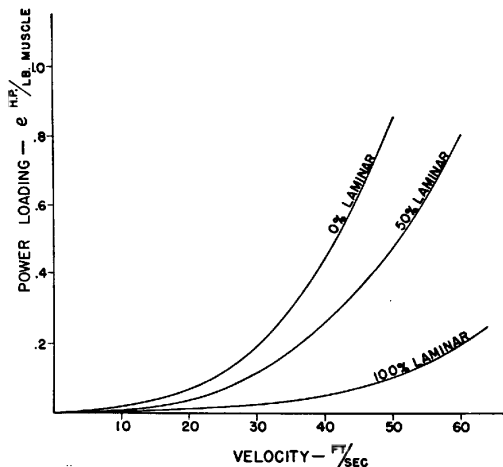


FIG. 18. Power loading versus steady-state velocity for barracuda no. 24, with per cent laminar flow as parameter. $\eta = 1.00$. See table 2.

Figure 18, which summarizes the barracuda study, indicates that for values of 40 feet/second, which were actually measured, values of $e = 0.15$ to $e = 0.20$ can be expected if the characteristic flow is 50 to 75 per cent laminar.

It appears that on the basis of the above analysis additional work should be initiated to investigate the physiological processes of the subject animals in order to define more accurately the limits of power loading. At the same time further hydrodynamic work should be initiated to determine the manner in which it becomes possible for these animals to obtain such favorable flow conditions and corresponding low drag values.

PROPELLSIVE EFFICIENCY

Propulsive efficiency as previously defined is construed for the present purpose to mean the efficiency with which the subject

animals convert the tail energy into forward thrust. The state of development of the general problem of fish propulsion has not progressed to the point where an exact experimental or analytical analysis can be made. Experimentally, one immediately becomes involved in food energy intake, basal metabolism, and such subjects, which in themselves are not as yet clearly defined. The large number of variables and unknowns involved in a completely analytical solution cast a very dubious shadow on the results of such an analysis.

The phases mentioned above having been evaluated, there appears to be one method, semi-empirical, that represents a

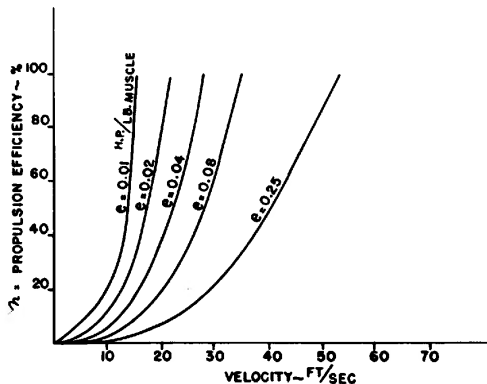


FIG. 19. Propulsive efficiency versus steady-state velocity for porpoise, with power loading as parameter. $m = 0$ per cent laminar. See figure 17 for porpoise characteristics.

logical beginning for an analysis of this type. This does not yield exact efficiency values but rather indicates what values must be obtained to satisfy known or approximated conditions.

Equation 21 can be rewritten and used for this purpose, since it involves all the important variables. In its revised form it becomes:

$$\eta = [0.00214 V^3 S / e W_m] [(1 - m/100) C_{f_T} + m/100 C_{f_L}] \quad (19)$$

The porpoise mentioned above was used as an example for this analysis. The results have been summarized and are presented in figures 19, 20, and 21 for $m = 0$ per cent, 50 per cent, and 100 per cent laminar flow conditions, respectively. Each figure represents η versus velocity, with e as a parameter.

If it is assumed that the porpoise tail is as efficient as a conventional propeller, with $\eta = 75$ per cent, several interesting observations can be made. From figures 19, 20, and 21 at 40 feet/second the power loadings must be 0.175, 0.08, and 0.017, respectively.

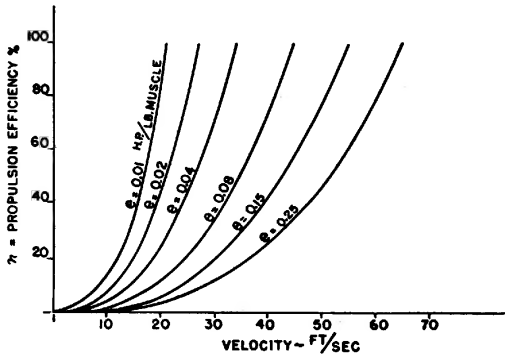


FIG. 20. Propulsive efficiency versus steady-state velocity for porpoise, with power loading as parameter. $m = 50$ per cent laminar. See figure 17 for porpoise characteristics.

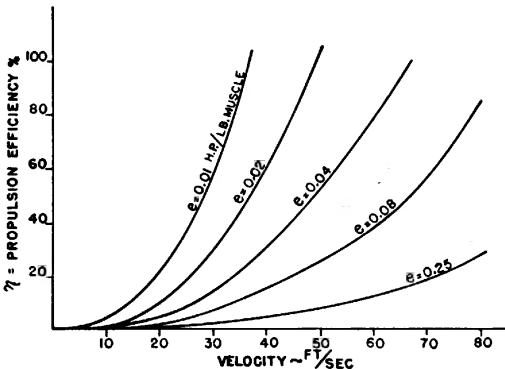


FIG. 21. Propulsive efficiency versus steady-state velocity for porpoise, with power loading as parameter. $m = 100$ per cent laminar. See figure 17 for porpoise characteristics.

These results in effect substantiate the previous conclusions, with the most reasonable condition being a 50 per cent laminar flow, with $e = 0.08$.

Second, for $V = 40$ feet/second, with $e = 0.01$, which is the presently accepted value, the efficiency must be greater than 100 per cent for any flow condition, which is not possible.

Therefore, it is apparent that reasonable efficiencies can be obtained only by an increase in presently accepted power loading values coupled with the presence of flow conditions of approximately 50 to 75 per cent laminar.

SUMMARY

The information presented here represents a summary of the more important aspects of the theoretical and experimental work carried on by the Goodyear Aircraft Corporation in connection with the study of the general problem of fish propulsion. Although the work has been of a research nature and in certain phases needs further substantiation, enough information is available to indicate that a further complete and comprehensive study of large salt-water fish should yield most valuable results.

The primary purpose of this program has been to determine whether or not there were any "secrets" that might be learned from fish that could be used for the improvement of under-water and lighter-than-air craft. The phase of the program completed thus far has been successful in this respect, since it can be seen from the information presented in the preceding paragraphs that for the fish to perform its normal functions satisfactorily certain physiological and hydrodynamic conditions must be satisfied that represent a considerable improvement over the presently accepted values of e (horsepower/pound muscle) and C_D , (total drag coefficient). In order to obtain physiological and hydrodynamic compatibility, it is necessary that the present e values be improved considerably and that some rational hydrodynamic explanation be provided that will permit fish to swim consistently in a regime of 50 per cent to 75 per cent laminar flow.

CONCLUSIONS

1. The determination of the drag of the fish and the subsequent substantiation of power loading e (horsepower/pound muscle) has been, in the past, based purely on the skin friction drag, with no consideration given to any other form of resistance. This practice is in error and has led to erroneous conclusions.

2. Presently accepted power loading values and drag coefficients are incorrect, and some compromise must be reached. Reasonable propulsive efficiencies can be obtained only by an improvement in power loading accompanied by a decrease in the total drag coefficients.

3. The improvement in power loading must be accomplished through a physiological approach, while the drag improvement can be realized only by further analyzing the hydrodynamics of the "real swimmers," such as tuna, which were not available for the above program.

BIBLIOGRAPHY

BREDER, C. M., JR.
1926. The locomotion of fishes. *Zoologica*, New York, vol. 4, pp. 159-297.

COHEN, A.
1933. Differential equations. New York, D. C. Heath and Co.

DICKINSON, S.
1928. The dynamics of bicycle pedalling. *Proc. Roy. Soc., London*, ser. B, vol. 103, pp. 225-233.

GRAY, J.
1936. Studies of animal locomotion. VI. The propulsive powers of the dolphin. *Jour. Exp. Biol.*, vol. 13, pp. 192-199.
1948. Aspects of locomotion of whales. *Nature, London*, vol. 161, pp. 199-200.

HILL, A. V.
1949. The dimensions of animals and their muscular dynamics. London, Royal Institute of Great Britain.

LANE, F. W.
1941. How fast do fish swim? *Country Life*, pp. 534-535.

MISES, R. von
1945. Theory of flight. New York, McGraw-Hill Publishing Co.

OKADA, MITUYO
1929. On the action of electric current on fishes. I. Excitation and narcosis. *Jour. Imp. Fish. Inst., Tokyo*, vol. 24, pp. 64-72.

PARRY, D. A.
1948. Aspects of locomotion of whales. *Nature, London*, vol. 161, p. 200.

RICHARDSON, E. G.
1936. The physical aspects of fish locomotion. *Jour. Exp. Biol.*, vol. 13, pp. 63-74.

SCHOLANDER, P. F.
1940. Experimental investigations on the respiratory function in diving mammals and birds. *Hvalrad. Skr.*, no. 22, pp. 1-131.